*Arab J. Nucl. Sci. Appl., Vol. 53, 1, 97-109 (2020)*

*Arab Journal of Nuclear Sciences and Applications*

**ISSN 1110-0451** ***Web site: ajnsa.journals.ekb.eg*** **(ESNSA)**

# A Mathematical Model for Studying the Effect of the Atmospheric Boundary Layer on the Surface Ozone Variations at a Coastal Site

**I. I. Bashter[a], M. A. Lasheen[b], E.M. Ahmed[c], O.S. Ahmed[d], A.A. El-Ghazaly[b]**

*[(1)]Physics Department, Faculty of [(a)] Department of physics, Faculty of Science, Zagazig University*

*[(b)] Nuclear Research Center, Atomic Energy Authority*

*[(c)] Faculty of Science, Princess Norah Bint Abdulrahman University*

*[(d)] Nuclear and Radiological Regulatory Authority*

**Received 25th Apr. 2018**
**Accepted 2nd Dec. 2019**

**Atmospheric Boundary Layer (ABL) height (h) is one of the basic criteria for describing its structure. ABL measurements, parameters and predictions have numerous practical and theoretical implementations as forecast of pollutant concentrations, surface temperature, expansion of disturbance measurements or in climate models and numerical weather prediction. The height of the mixing layer is difficult to be measured; therefore, mathematical methods are introduced to calculate this layer and different FORTRAN programs have been developed to define the height of ABL on an hourly basis through the year. The analysis of the results showed that the variation of the height of the mixing layer for different seasons depends on the type of the dominant stability class and the value of wind speed, where the rise of the mixing layer in winter and autumn months may be related to increased frequency of stability conditions in the unstable and slightly unstable atmosphere On the other hand, when the stable conditions are dominant, the height of the mixing layer remains smaller.**

**The boundary layer ozone is a standard contaminant because of its harmful effects on living organisms and plants. It also has an active role in atmospheric chemistry and climate change; therefore, monthly and seasonal variation of the surface ozone $O_3$ concentration and its effects on the atmospheric boundary layer are measured for the first time at a coastal site in Egypt in the year 2013.**

**Keywords:** *Atmospheric boundary layer / Mixing height / Modeling / Surface ozone $O_3$*

## Introduction

The complexity of the various processes affecting on the concentrations of pollutant indicates the necessity for the use of dispersion models. The main keys introduced in these models are the meteorological measurements, fields and parameters needed to calculate the transport, dispersion and removal of contaminants. The dispersion and removal of contaminants (by dry precipitation) are based on turbulence of the atmosphere, but meteorological services do not routinely monitor and measure these turbulence. Therefore, the dispersion characteristics of basic meteorological parameters such as wind, temperature and radiation are derived using descriptive schemas or are determined with specific models [1].

The ABL is the layer where interactions take place between the earth's surface (which captures most of the incoming solar energy and redistributes it in different forms) and the large-scale atmospheric flow (which is driven by this energy).

Materials released into the atmospheric layer (ABL) are progressively dispersed horizontally and vertically over turbulence, and eventually become fully intertwined above this layer if enough time is given and if there are no considerable sinks. Therefore, it became common in meteorological air pollution to use the term mixed layer or mixing layer.

Corresponding author: ahmadysci@yahoo.com
DOI: 10.21608/ajnsa.2019.12283.1210

Mixing layers set the volume obtainable for dispersion of pollutants and also contribute in many predictive and diagnostic processes and / or models for assessing concentrations of pollutants near the surface

This transfer of energy is partly accomplished by turbulent eddies. The ABL transfers not only sensible and latent heat, but also momentum and atmospheric constituents between the surface and higher atmospheric levels. This transfer of properties in the ABL is thus primordial for the dispersion of pollutants emitted mostly within the ABL. Moreover, the great importance of the exchange of many traces constituents (e.g., SO2, NOx, O3, CO2, CH4 which are often emitted into or deposited from the atmosphere to terrestrial and aquatic ecosystems via the ABL has been recognized as one of the main links in global biogeochemical cycles. It is thus of primary importance to be able to understand, measure, parameterize, simulate and predict the structure and behavior of the ABL [2].

The height (h) of the ABL is an important parameter in dispersion modeling. Ozone of the boundary layer is a standard pollutant because of its harmful effects on living organisms and vegetation and has a major impact on atmospheric chemistry and climate change.

**Methodology**

Determination of the height (h) of ABL is the subject of this study. The study area is located on the north coast on the Mediterranean Sea. The regional location of the study area is shown in Fig. (1) [3]. The site area lies in the western desert, directly overlooking the sea and is located between 310 30' - 310 28' North and between 260 45' - 260 35' East.

Geographically, the study area in north of Al-Mathany village, Mersa Matruh governorate, which is located at about 50 km west of Mersa Matruh, 290 km west of Alexandria, and 25 km east of Al Nigilla village. Cairo is approximately 400 km southeast. The site extends over the Northern Coast by approximately 6 km, while the width 5 km to the south. The only large locality is Mersa Matruh governorate.

Figure (2) presents the analysis of the whole year 2013 by WRPLOT code [4], which shows that the North North West direction sector (NNW) is the prevailing wind direction, and North West direction sector (NW) is the second predominate sector. Therefore, the two sectors South South East (SSE) and Southeast (SE) are the two prevailing downwind sectors. In general, the speed of the wind ranges between moderate and slow along these directions.

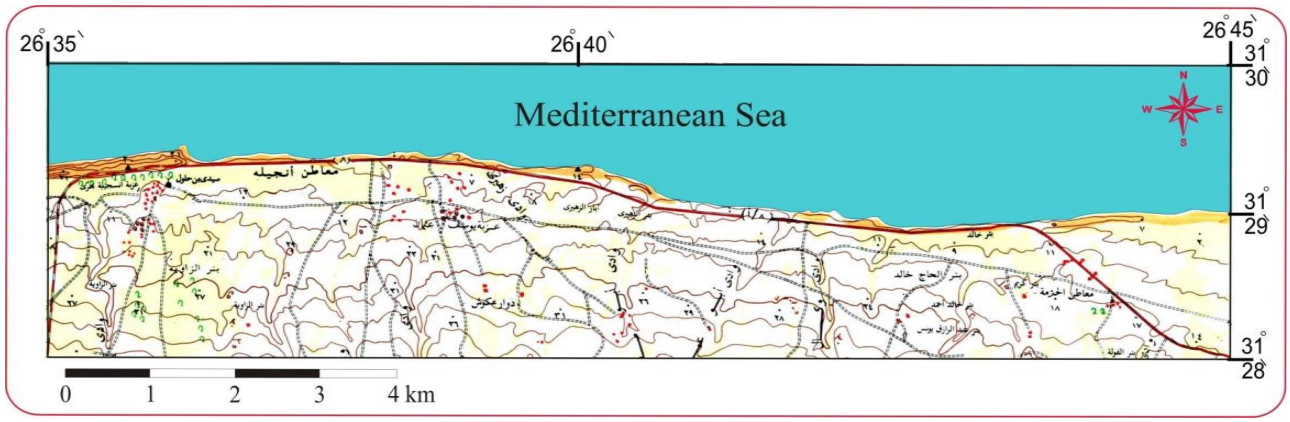


**Figure (1): the map of the selected area, Egypt (lasheen, 2013)**

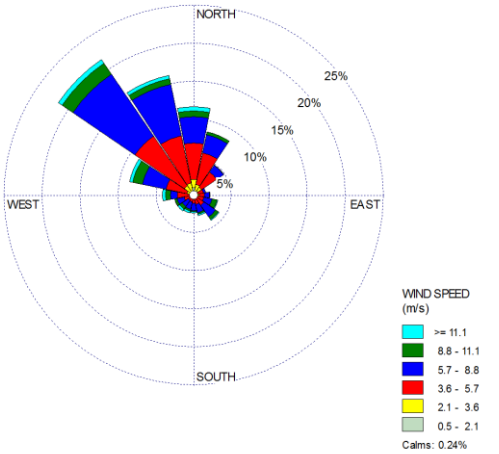


**Figure (2): Annually wind rose of one complete year (2013)**

*Theoretical background*

Numerous computer models have been developed to predict dispersion of pollutants. Most models rely on empirical formulas, despite the development of computer processors and complex numerical algorithms, which are input to wind flow or make some approximate calculations and then use statistical correlation to predict the dispersal of pollutants [1].

A FORTRAN computer program was developed to estimate the height of the ABL for different seasons. This method used several meteorological factors gathered with the National Oceanic and Atmospheric Agency, US website [5] such as wind speed, temperature and stability class for different seasons of one complete year 2013. Stability classes can be divided into the following classes; A- Extremely unstable, B- Moderately unstable and C- Slightly unstable [6]. Each one of them has a direct impact on the height of ABL.

*Neutral conditions*

For neutral conditions, the ABL heights were calculated by the use of the following equation [7];

$$h_n = C_n U^* / f \quad (1)$$

Where;

**$h_n$** the height of the ABL in case of neutral condition

**$C_n$** is the proportionality constant and equal 0.2

**f** is the Coriolis frequency which equal 2Ω sin φ, Ω is the earth rotation rate, φ is latitude geographic coordinate of the study area = 31º 29"

**U*** is the friction velocity and given by the following equation;

$$U^* = k\,u\,[\ln (Z/Z_o)]^{-1} \quad (2)$$

Where**;**

**k** Von Karman constant equal to 0.4

**u** the wind velocity at height equal Z

**Z** the reference height at 10 m

**$Z_o$** the roughness height = 0.03 m

*Stable condition*

For stable condition, the ABL heights were calculated by using the following expression [7];

$$h_S = C_S\,[U^* L/f]^{1/2} \quad (3)$$

**Where;**

**$h_s$** the height of the ABL in case of stable condition

**$C_S$** is the structure parameter for the variable S and equal 0.4

**$U^*$** is the friction velocity in case of stable condition, which is given by the following equation;

$$U^* = k\,u\,[\ln(Z/Z_o) + 5\,(Z/L)]^{-1} \quad (4)$$

**L** is the length of Monin-Obukhov, which characterize the effects of buoyancy on turbulent flows, especially in the lower tenth of the air boundary layer [8].

*Unstable conditions*

The heights of the ABL was controlled by convective eddies for unstable condition. The

evaluation of the convective ABL is determined by applying the following equation [7];

$$\frac{dh}{dt} = \left[\left((1+2C_1)(w'\theta'_o)\right)/\Gamma h\right] + \left[C_2 (U^{*3}/\Gamma\beta h^2)\right]$$

By solving this equation, we get;

$$h^3 = 3(1+2C_1)(w'\theta'_o)\, t\ h/\Gamma + 3C_2 U^{*3} t/\beta\Gamma$$

Where,

The friction velocity is given by the following equation:

$$U^* = k u \left[\ln\left(Z/Z_o\right) - 2\ln\left(0.5\left(1+\frac{1}{\phi_m}\right)\right) - \ln\left(0.5\left(1+\frac{1}{\phi^2_m}\right)\right) + 2\tan\left(\frac{1}{\phi_m}\right) - \left(\frac{\pi}{2}\right)\right]^{-1}$$

$$\phi_m = \left(1-15\left(\frac{Z}{L}\right)\right)^{-1/3}$$

**h** is the height of the ABL in case of unstable condition

**$C_1$, $C_2$** are constants and equal to 0.2 and 2.5

**$w'\ \theta'_0$** is the entertainment heat flux and equal to $U^{*3}/k\beta L$

**Γ** is the potential temperature gradient above the inversion layer and equal to 0.005

**$\phi_m$** buoyancy parameter = g /$\theta$ where, g is the gravity = 9.8 m/s$^2$ and θ is the potential temperature at Z height

The Monin-Obukhov length in case of unstable conditions can be determined using the following equation [9];

$$L^{-1} = a\ Z^b$$

Knowing the stability classes, the identical length scale of Monin-Obukhov will be measured at given Z. The constants (a, b) based on the stability classes and are shown in Table (1).

**Table (1): The constants (a) and (b) at different stability classes**

| Constants | Stability classes | | |
|---|---|---|---|
| | **A** | **B** | **C** |
| **a** | - 0.0875 | - 0.03849 | - 0.00807 |
| **b** | -0.1029 | -0.1714 | -0.3049 |

**A, B, C:** unstable conditions

## Results and discussion

*Stability class*

From Figure (3), it was observed that the neutral stability category (D) is predominant in this region, where the neutral ratio in winter is 76.47%, but the unstable state is 5.23% and the steady state is 3.93%. In the spring, the neutral container reaches 57.93%, but the unstable situation is 10.79% and the steady state is 4.85%. In the summer, the neutral container reaches 56.85%, but the unstable state is 10.57% and the steady state is 5.73%. In the end, in the autumn, the neutral, unstable and stable state is 68.00, 5.68 and 7.48% respectively.

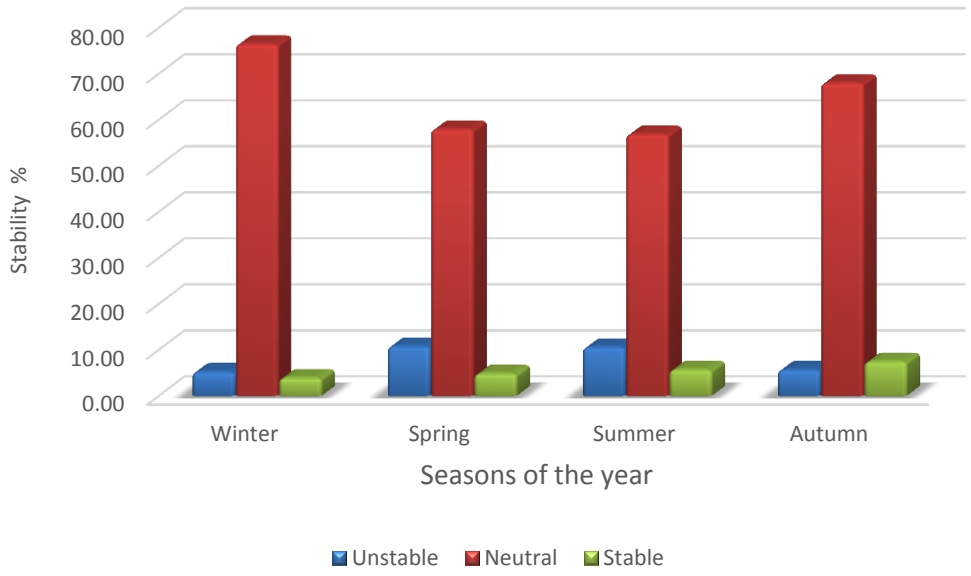


**Figure (3): Stability class for seasons of the year 2013**

*Mixing height layer*
The seasonal and monthly height of mixing layer during the year 2013 for the study area will be discussed as follows:

*Winter*
From Figure (4), it is noticed that the height of the mixing layer for months January, February and March reaches its maximum value 2403 m in February month from wind speed equal 6.4 m/s due to the nature of atmosphere and incoming solar radiation.

*Spring*
Figure (5) indicates that the height of mixing layer (ML) for months April, May and June reaches its maximum value of 1882 m in April from wind speed of 6.2 m/s due to the nature of atmosphere and incoming solar radiation.

Summer
As shown in Figure (6), the height of ML for the months July, August and September reaches its maximum value (2581 m) in July from wind speed of 6.1 m/s due to the nature of atmosphere and incoming solar radiation.

Autumn
From Figure (7), it is noticed that the height of ML for months October, November and December reaches its maximum value (2799) m in December from wind speed of 6.7 m/s due to the nature of atmosphere and incoming solar radiation.
There is a strong relation between the effects of some meteorological parameters on the mixing layer height such as temperature, wind speed and relative humidity. Therefore, the influence of these parameters is studied in the following section.

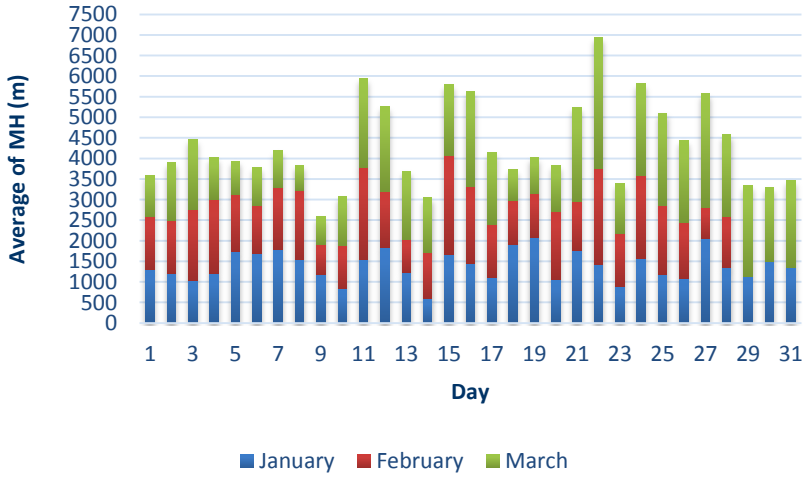


**Figure (4): Average of mixing height layer in winter season**

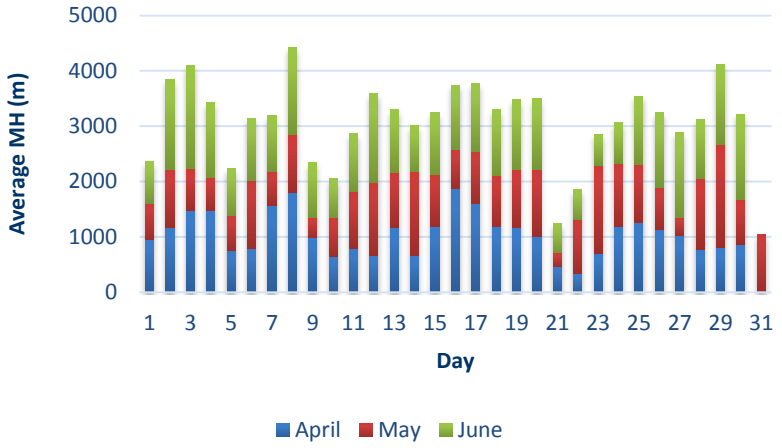


**Figure (5): Average of mixing layer height in spring season**

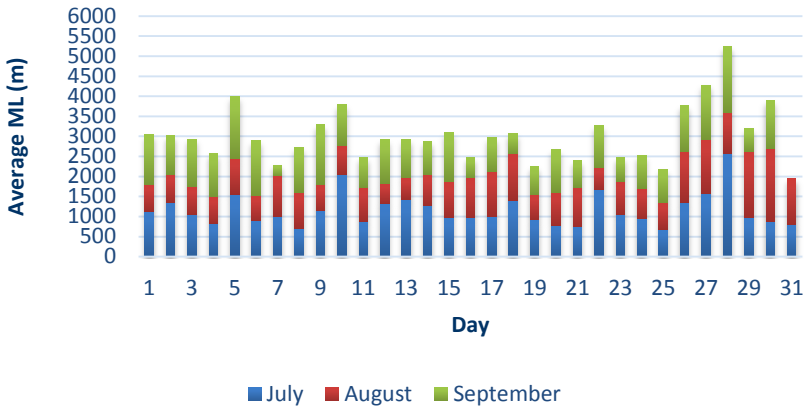


**Figure (6): Average of mixing layer height in summer season**

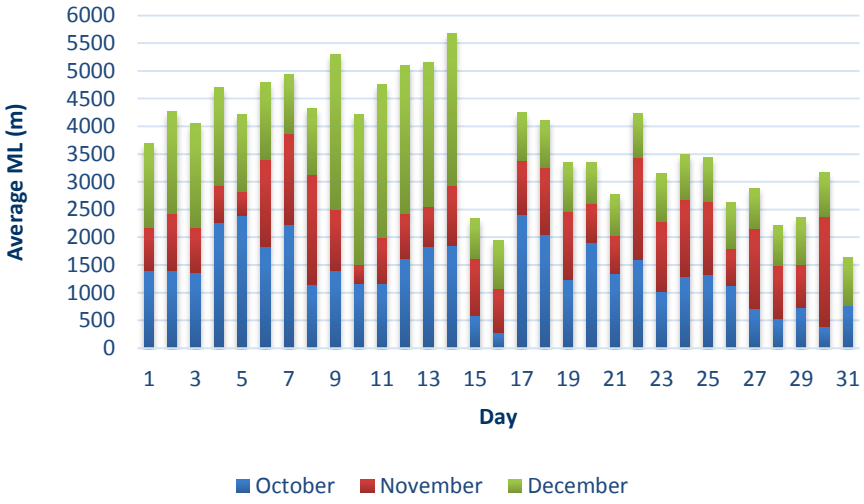


**Figure (7): Average of mixing layer height in autumn season**

*Meteorological parameters effect on afternoon mixing height*

The average monthly difference of the maximum mixing height and values identical to the estimated temperature, relative humidity and wind speed at noon of the year 2013 are shown in Figure (8) and Table (2). The results show that the minimum monthly mean values of MH takes place in hot months, particularly in August (888 m), however the maximum values in the cold months, particularly in March (1535 m).

Affirmative correlation was found between the maximum of monthly mean of wind speed and relative humidity. While, negative correlation was found between temperature and relative humidity.

The average monthly T value is minimum in the cold months, January ($14^0$ C) and February ($15^0$ C), the maximum is reached in hot months, August ($27^0$ C) and September ($26^0$ C). The average monthly value of RH reaches the minimum value of March (62 %) and October (64 %), the maximum in July (78 %) and August (76 %). Average monthly WS value is the minimum value in November (4.7 m/s), August (5.1 m/s), maximum in March (7.1 m/s), and January (6.9 m/s).

Rising atmospheric temperature corresponds to strong solar radiation and respective atmospheric turbulence, Furthermore, increasing the frequency atmospheric stability of unstable and slightly unstable cases in the months of winter and autumn contributes significantly to the increase in mixing height.

**Table (2): Monthly average values of maximum MH and corresponding values of T, RH and WS at afternoon time**

| Month | MH (m) | T ($^0$C) | RH (%) | WS (m/s) |
|---|---|---|---|---|
| **January** | 1387 | 14 | 69 | 6.9 |
| **February** | 1452 | 15 | 65 | 6.4 |
| **March** | 1535 | 17 | 62 | 7.1 |
| **April** | 1043 | 18 | 67 | 6.2 |
| **May** | 967 | 23 | 67 | 5.2 |
| **June** | 1068 | 24 | 73 | 6.4 |
| **July** | 1095 | 25 | 78 | 6.1 |
| **August** | 888 | 27 | 76 | 5.1 |
| **September** | 988 | 26 | 69 | 5.4 |
| **October** | 1289 | 23 | 64 | 6.1 |
| **November** | 1051 | 20 | 69 | 4.7 |
| **December** | 1534 | 15 | 73 | 6.7 |
| **Max** | ***1535*** | ***27*** | ***78*** | ***7.1*** |
| **Min** | ***888*** | ***14*** | ***62*** | ***4.7*** |

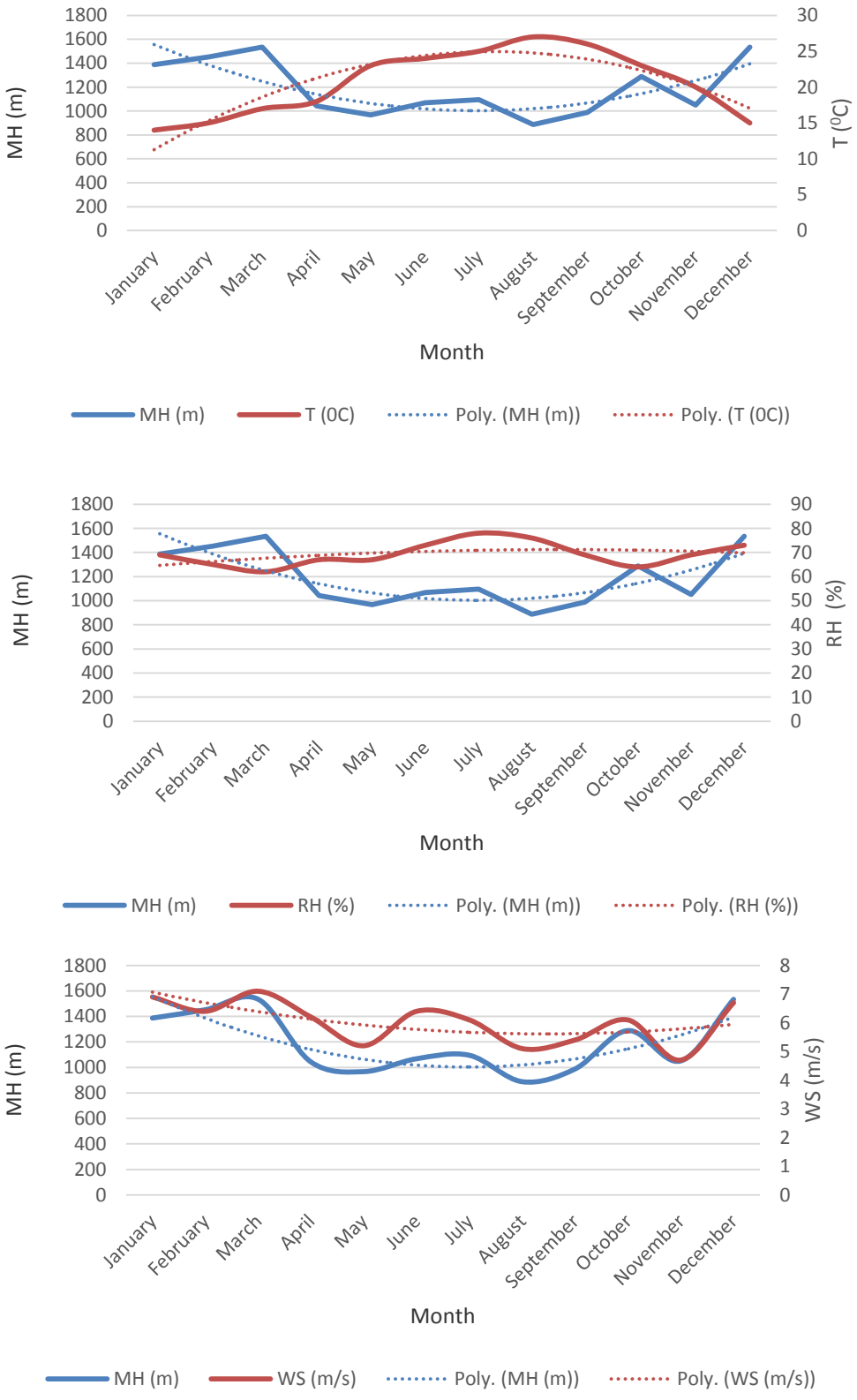


**Figure (8): Monthly average values of maximum MH and corresponding values of T, RH and WS at afternoon time**

In spring and summer months, there is an increase in the mixing height as a result of a strong mechanical turbulence that takes place due to the rise of the wind speed. While a decrease in the value of mixing height was observed due to the stability of the atmosphere.

*Atmospheric boundary layer and effects on the surface ozone*

One of the most important parameters that is pertinent to study the air pollution in detail is the Convective Boundary Layer (CBL) height, where the volume of the atmosphere is measured in which different pollutants are mixed and their precursors. The contribution of diurnal variation in the boundary layer height is considered in deciding the air-quality standard during different times of the day. Therefore, simultaneous observations of trace species and the evolution of the boundary layer are necessary to study these aspects [10].

Ozone in the boundary layer is a standard contaminant because of its harmful effects on living organisms and plants so; it is a significant factor in the changes of atmospheric climate. The tropospheric ozone main source is photo-oxidation of some of the pollutants including CO, methane and other Hydrocarbons in an adequate quantity of $NO_x$; it is a general expression for nitrogen oxides most relevant to air pollution. These gases are the main cause of the tropospheric ozone, in addition

to the formation of acid rain and smog. Another source of tropospheric ozone is the downward transport of ozone-rich air from the stratosphere. Among these two sources, photochemical in situ appears to have a predominant contribution especially in the boundary layer [11].

*Method and unit*

Using UV (ultra-violate) analysis, surface ozone $O_3$ is determined by a light absorption analysis method. The observation category is air sampling observation at a stationary platform. Also, the measurement unit used is ppb.

Figure (9) shows the monthly variation of the surface ozone $O_3$ concentration, where, the maximum $O_3$ concentration occurs in July, with value of 33.827 ppb and the minimum in January of a value of 5.437 ppb. Figure (10) presents seasonal variability of surface ozone at the coastal site. It is cleared that in the summer season the concentration of $O_3$ is high with an average value of 26.16 ppb, and this concentration is low (9.08 ppb) in the winter season.

The explanation for increasing ozone concentration gradually is due to sunrise due to the fact that photochemical reactions are dominant only in the presence of sunlight and because of the high density of solar flow during the summer the maximum surface ozone value is recorded. On the contrary, ozone levels are lower in winter. It can be proved that there is a strong correlation between temperature of surface and photochemical production of surface ozone [12].

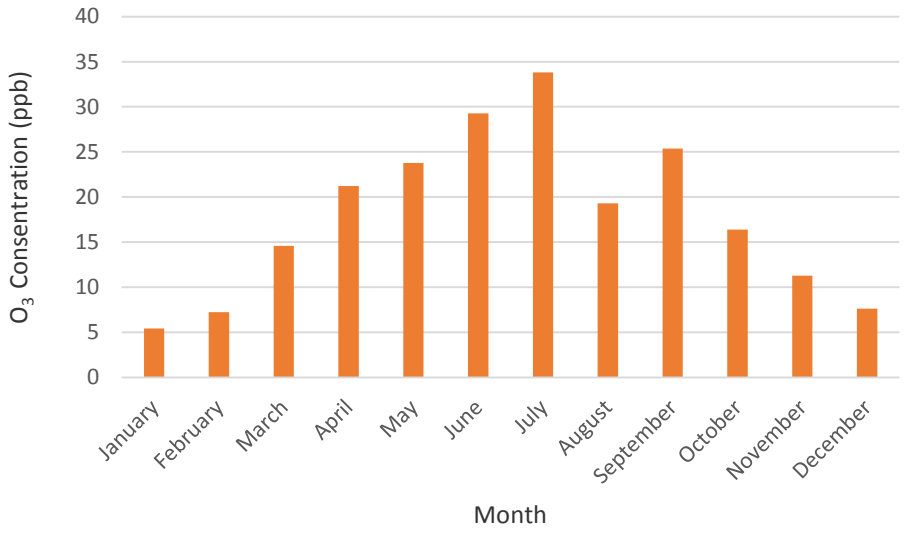


**Figure (9): Monthly variation of $O_3$ for the full year, (2013)**

*Diurnal variation in ozone*

Figure (11) shows the average diurnal variance of surface ozone through the month of June. Photochemical production of ozone is an effective factor in the high levels of ozone in the daytime, while the surface ozone at night is significantly reduced; this is mainly due to ozone calibration by chemical analysis NO in the shoal boundary layer [12].

Besides the role of photochemistry, meteorology and border layer dynamics, they are major causes of ozone variability [13-14]. After sunrise, the Boundary layer gradually reaches maximum altitude during the afternoon hours because of the increased heating of the surface. As time passes and the trace species are closely mixed within, convective mixed layer is formed. Figure (13) indicates the daytime $O_3$ concentrations cycles in November, 2013.

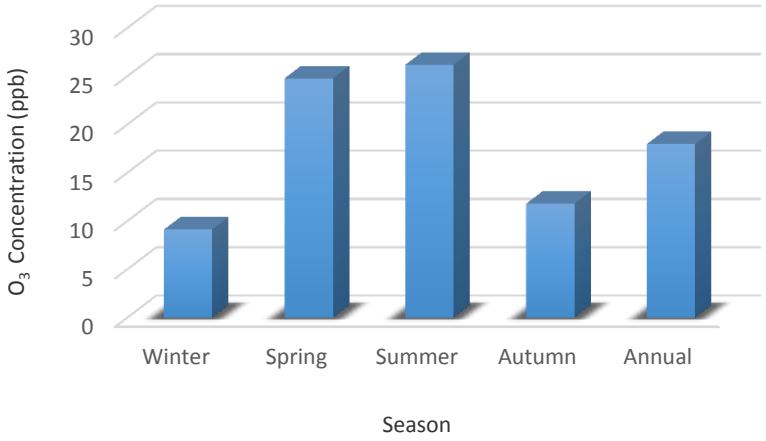


**Figure (10): Seasonal variability of surface ozone at coastal site**

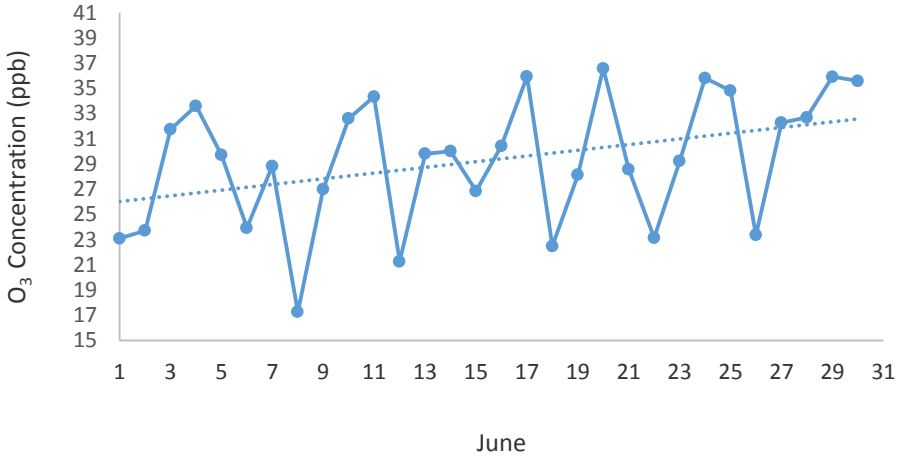


**Figure (11): Monthly average ozone diurnal variations during June, 2013**

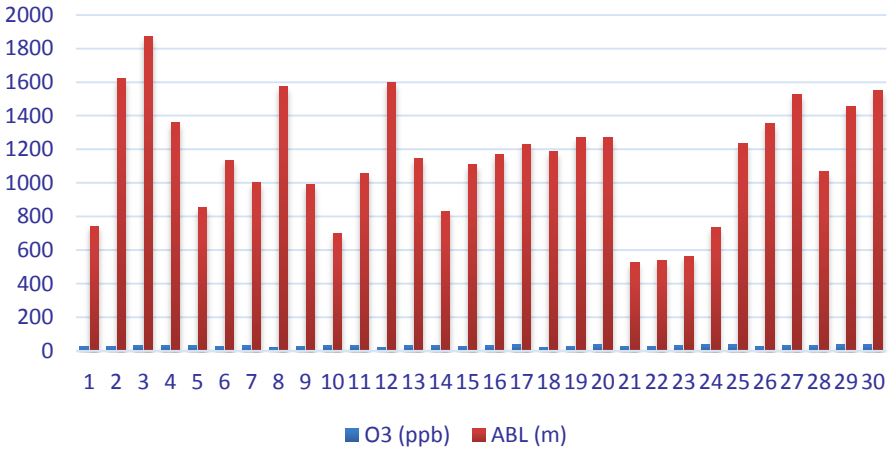


**Figure (12) Distribution of $O_3$ concentration and atmospheric boundary layer in June, 2013**

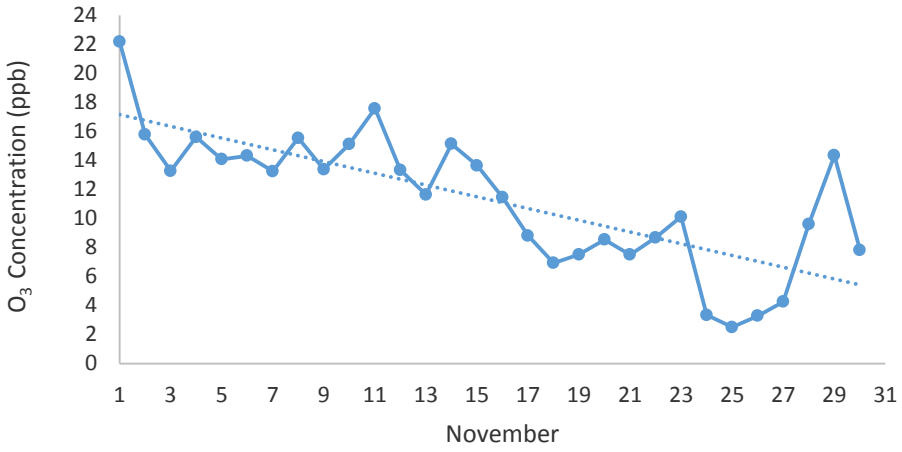


**Figure (13): Monthly average ozone diurnal variations during November, 2013**

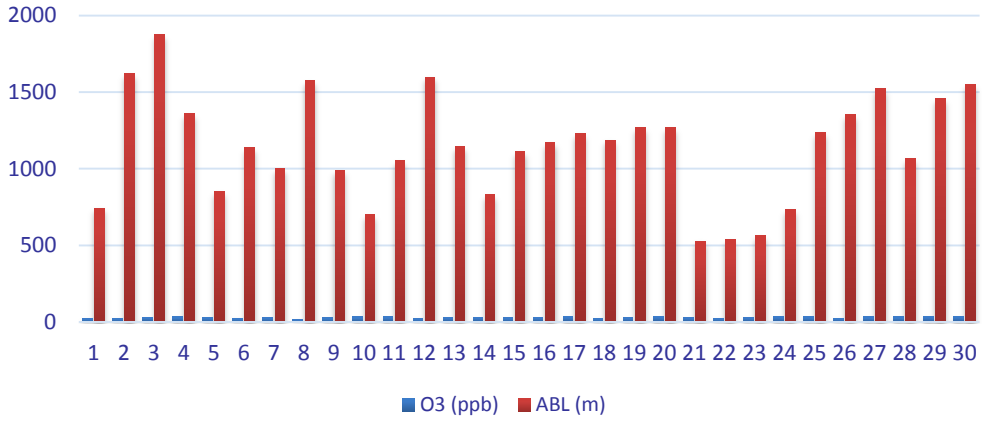


**Figure (14): Distribution of $O_3$ concentration and atmospheric boundary layer in November, 2013**

Figure (15) shows both the height of the boundary layer and the ozone mixing ratio decreases from 1 to 5, 8 to 10 and from 23 to 26 November. Both are also found to be ascending from 10 to 11, from 13 to 14, from 21 to 22 and from 26 to 27 November.

The lowest rates of ozone mixing are observed on a rainy day (25 November) when the height of the boundary layer is also lower, which is about 1320 meters. In general, rainfall associated with cloudy conditions reduces solar radiation, which reduces the production of photochemical ozone. In addition, the rise of the lower layer increases the loss of ozone by deposition of the surface, and the rise of the lower layer reduces the mixing of the poor air mass in ozone on the surface with the ozone-rich air mass at higher altitudes.

**Conclusion**

Atmospheric boundary layer is highly correlated with stability class and some meteorological parameters where, the average monthly values for maximum mixing height were high during the hot months, especially in August (888 m). However the maximum values in the cold months take place especially in March (1535 m). A positive correlation was found between the monthly averages for maximum mixing and wind speed, at the same time, there is a negative association with both of temperature and relative humidity.

The boundary layer reaches the maximum height during the afternoon due to increased surface heating. At this time, the trace species are strongly mixed within, consequently forming a convective mixed layer. The lowest values in the morning are the result of the ozone destruction process at night, including loss due to atmospheric chemistry and dry deposition on the ground. The observed increase in the afternoon hours is due to the predominance of photochemical production in the highly conductive weather.

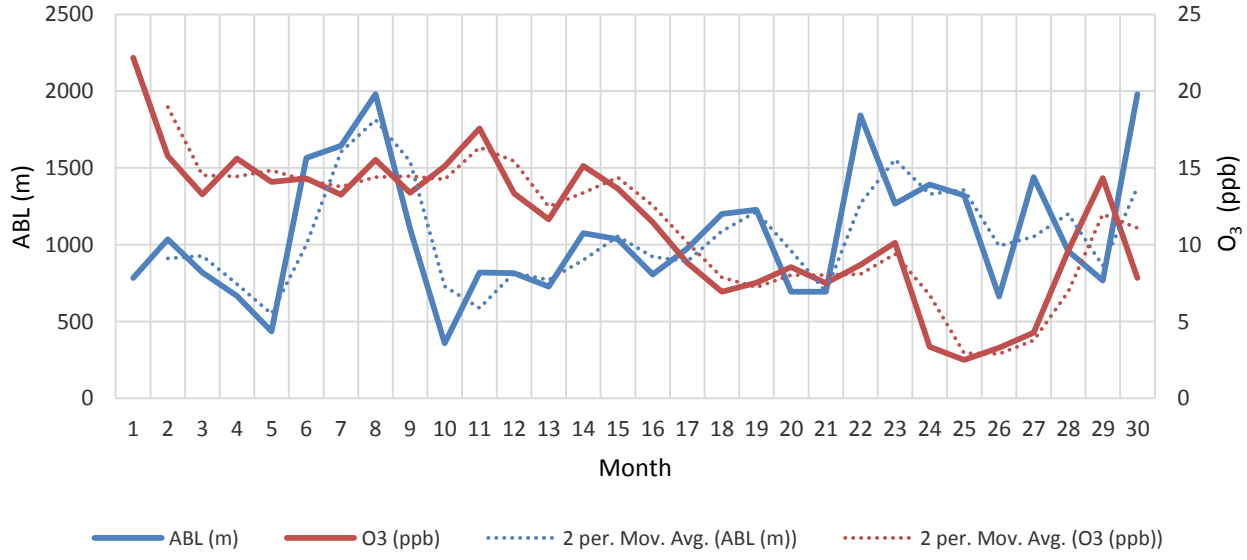


**Figure (15): Atmospheric boundary layer height and ozone mixing ratios**

**References**

1-Fisher, B., Erbrink, J., Finardi, S. (1998) Harmonization of the Pre-processing of Meteorological Data for Atmospheric Dispersion Models, Cost Action 710, *Final Report*. Eds. Ec Belgium.

2- Stull, R. B. (1988) An Introduction to Boundary Layer Meteorology, Dordrecht- Boston- London: *Kluwer Academic Publishers*, 665.

3-Lasheen, M. A. (2013) Modernization of Background of Natural Radioactivity in North Western Coast, Egypt, *M. Sc, Thesis*, Physics department, Faculty of Science, Zagazig University.

4-Jessel, L., Cristiane, L., Michael, A., Johnson, O., Shatalov, O. (1998-2011) WRPLOT View, Wind Rose Plots for Meteorological Data, Version 7.0.0, (c), *Lake Environmental Software*, http://www.weblakes.com/

5- NOOA, National Oceanic and Atmospheric Agency, US. website: http://www.noaa.gov/

6-IAEA (1980) Atmospheric Dispersion in Nuclear Power Plant Siting. *A Safety Guide*, Safety Series No. 50-Sg-S3.S

7-Sugiyama, G., Nasstrom, J.S. (1999) Methods for Determining the Height of the Atmospheric Boundary Layer. US, Department of Commerce, 5285 Port Royal Rd., *Springfield*, VA 22161.

8-Hanna, S. R., Burkhart, C.L., Paine, R. G. (1985) Mixing Height Uncertainties. *Proc. 7th AMS Symp. Turb. & Diff, Boulder*, 82-85.

9-Zannetti, P. (1990) Air Pollution Modeling: Theories, Computational Methods and Available Software, Computer Mechanics, Publisher: *Van Nastrand Reinhold*, 60.

10-Aneja, V., Arya, S., Murray, C. Manuszak, T. (2000) Climatology of Diurnal Trends and Vertical Distribution of Ozone in the Atmospheric Boundary Layer in Urban North Carolina, *J. Air and Waste Manag*. Assoc, (50), 54–64.

11-Crutzen, P. J. (1995) Ozone in the Troposphere, in Composition, Chemistry, and Climate of the Atmosphere (ed.), *Singh H B, New York*, Vann strand Reinhold, 349-393.

12-Naja, M., Lal, S. (2002) Surface Ozone and Precursor Gases at Gandaki (13.5° N, 79.2° E), A tropical Rural Site in India, *J. Geophys. Res*. 107, doi: 10.1029/2001JD000357.

13-Banta, R., Senff, C., White, A., Trainer, M. (1998) Daytime Buildup and Nighttime Transport of Urban Ozone in the Boundary Layer During a Stagnation Episode, *J. Geophys. Res.* 103 (22), 519- 544.

14-White, A., Templeman, B., Angevine, W., Zamora, R. (2002) Regional Contrast in Morning Transitions Observed During the 1999 Southern Oxidants Study Nashville/Middle Tennessee Intensive. *J. Geophy. Res*. (107), 4726.